Available online at www.sciencedirect.com

ScienceDirect

Procedia Structural Integrity 42 (2022) 1483–1496

Structural Integrity Procedia

www.elsevier.com/locate/procedia

23 European Conference on Fracture - ECF23

Numerical simulation of 14Mov6-3 steel CT-specimen Fracture Behavior

Bojana ZEČEVIĆ [1], Ana MAKSIMOVIĆ[1] , Ljubica MILOVIĆ [2], Vujadin ALEKSIĆ[3], Aleksandar GRBOVIĆ[4], Srđan BULATOVIĆ[3]

[1]*University of Belgrade, Innovation Centre of the Faculty of Technology and Metallurgy, 4 Karnegijeva St, 11120 Belgrade, Serbia*
[2]*University of Belgrade, Faculty of Technology and Metallurgy, Belgrade, Serbia*
[3]*Institute for Testing of Materials-IMS Institute, Belgrade, Serbia*
[4]*University of Belgrade, Faculty of Mechanical Engineering, Belgrade, Serbia*

Abstract

Steel grade 14MoV6 3 is used for manufacturing of boilers and steam pipelines designed for steam temperatures up to 560 °C. This paper presents the numerical simulation of a CT-specimen, using the finite element method. The analysis was performed using Ansys Workbench R21, and represents the initial stage of extensive research involving the behaviour of 14MoV6 3 steel. The goal was to simulate the real experimental conditions, including boundary conditions and loads, which were defined in accordance with relevant standards, and to obtain representative results. The temperature dependent mechanical properties needed for the simulation of plastic behaviour of such specimens under tensile loads were obtained from the experimental data and the literature.

Keywords: Steam pipeline; CT-specimen; Finite Element Method.

1. Introduction

Application of the finite element method (FEM) is of particular importance in the field of fracture mechanics. It is possible to determine the life time of the structure based on the predefined geometry of the structure, the mechanical characteristics of the applied material, the position, geometry and dimension of the initial crack. This method made a significant contribution to the design of bearing elements of complex geometric shapes.

*Corresponding author. Tel.: +387645523025; fax: +387113370387.
E-mail address: baleksic@tmf.bg.ac.rs

2452-3216
10.1016/j.prostr.2022.12.189

FEM is often used while designing structures in the presence of a crack. In elastic-plastic fracture mechanics (EPFM), due to the non-linear behavior of materials, it is not possible to reach a solution in a closed form, so in addition to experimental research, the use of FEM in this area is considered to be a very important part of the procedure [1]. Crack modeling using FEM is efficient and cheap, but also problematic in terms of the required resources and the accuracy of the results, which depends on the elements' mesh that has been formed. Each new crack front requires the generation of a new finite element mesh, which complicates rather complex structure of the existing mesh. Therefore, it is necessary to re-generate the mesh in the vicinity of the crack tips, as well as its refinement to obtain the most accurate results. Mesh redefinition is done by the user of the software, which means that a high level of knowledge and professionalism is required from the one who create the finite elements mesh. [2, 3].
ANSYS is a commercial software for structural analysis using FEM. It offers users a large number of types of analysis with three-dimensional (3D) modeling of structures [4,5]. For the purposes of the research presented in this paper, the test specimen models were created in the commercial program CATIA v5 and then imported into ANSYS in which the value of the *J*-integral was calculated and the fatigue crack growth was simulated.

2. Calculation of the *J*-integral using FEM

All numerical simulations were performed in the Ansys Workbench R21 software package that relies on FEM. Two models of C(T) specimens for testing at elevated and room temperature were created in CATIA v5, whose geometries are shown in fig. 1 and 2. The models were then imported into Ansys Workbench, after which the finite element grid was generated, boundary conditions and loads were defined [6-11].

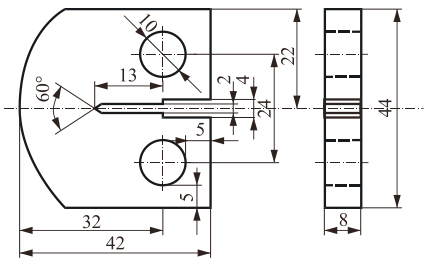

Figure 1. Modified C(T) test specimen for fracture toughness tests in a high temperature (HT) chamber

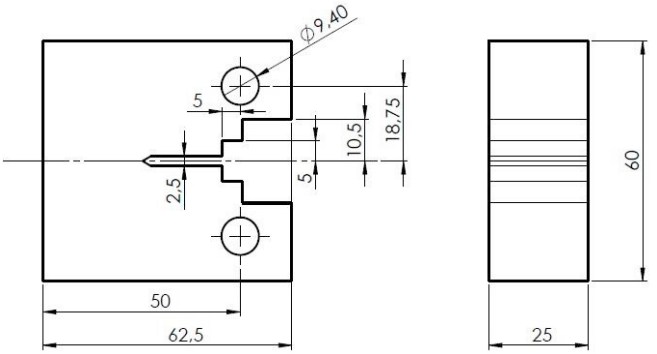

Figure 2. Step notch C(T) test specimen for fracture toughness tests at room temperature (RT)

2.1. Specimen for elevated temperature testing

The following figures show the steps of defining the FEM from the definition of the initial geometry, Figs. 1 and 3, through setting boundary conditions, entering loads and meshing, which led to obtaining a numerical model ready for calculation of the specimen which will be tested at 540 °C (HT. The size of the elements varied depending on their location, smaller elements were used in places where fatigue crack growth was expected, while larger elements were used in places far from the critical ones, in order to keep the number of nodes as low as possible, so that the calculation would be simplified to some extent. In all models, tetrahedral finite elements with 20 nodes were used, Fig. 4, where the total number of nodes for the model at elevated temperature is 64368, while the number of elements is 44559.

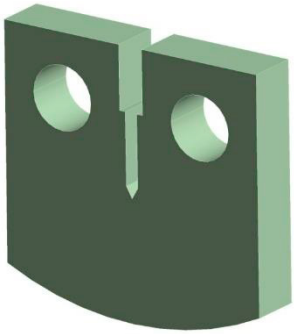

Figure 3. Geometry of the sample for testing at HT

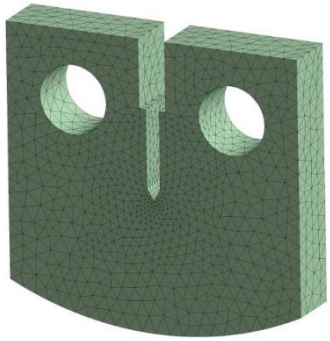

Figure 4. FE mesh

For the force value, the maximum value from the experiment F=5000 N was taken, Fig. 5. A detailed view of the boundary conditions: limited displacements in the y, x and z direction can be seen in Fig. 6.
Material properties were determined on the basis of experiments, tensile tests, for the parent material at operating and room temperature, while the mechanical properties were used to yield strength, ultimate tensile strength and elongation also measured in the experiment for the material at service and room temperature. Displacements of the specimen at the end of the process of numerical simulation of crack propagation is shown in Fig. 7.

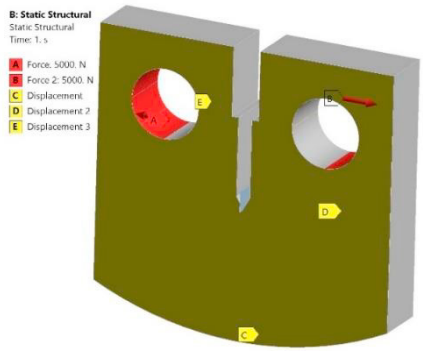

Figure 5. Boundary conditions - displacements (yellow color) and load in the form of forces (red color)

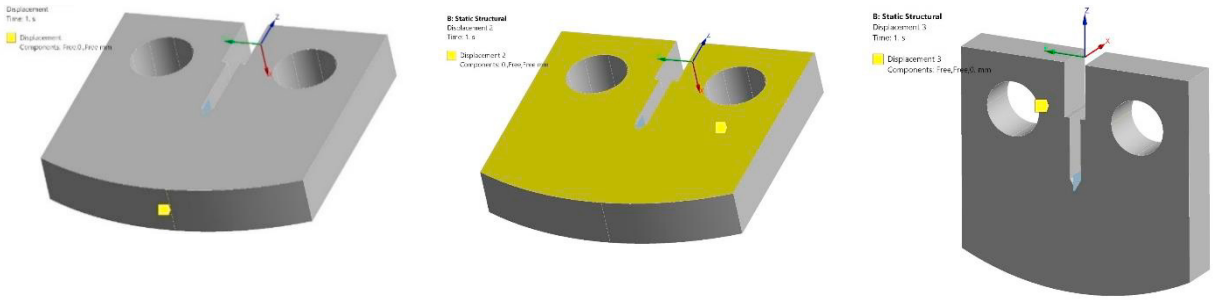

(a) (b) (c)

Figure 6. Detailed view of boundary conditions: constrained displacements in: (a) y, (b) x and (c) z direction

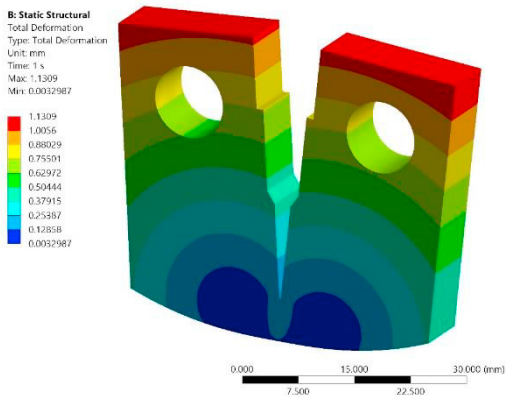

Figure 7. Specimen displacements in mm at the end of the process of numerical simulation of crack growth in the specimen at HT

The maximum stress was at the crack tip after opening the crack, Fig. 8, and at the end of the propagation simulation, Fig. 9, which was expected.

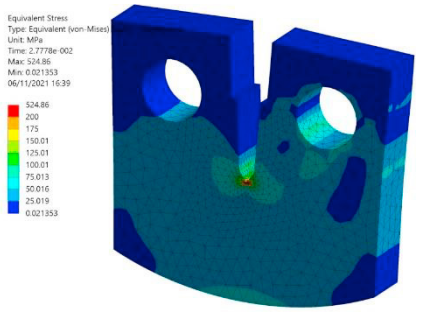

Figure 8. The stress state after opening the specimen crack at HT

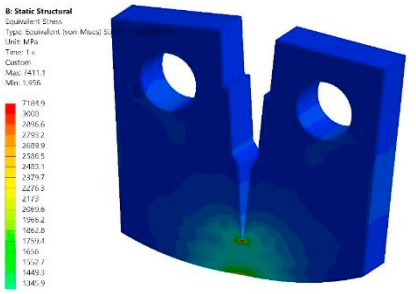

Figure 9. Stress state at the end of the specimen crack propagation simulation at HT

The *J*-integral value after crack opening and at the end of crack propagation simulation is shown in Fig. 10. The *J*-integral was calculated at the nodes of the crack tips, and looking at its values it can be seen that the crack grew in a plane.

The values of the critical *J*-integral cannot be calculated numerically, but its critical value can be estimated. The initial diagram for evaluation is diagram *a*-*N*, Fig. 11, where it is necessary to estimate the number of cycles for which the crack begins to grow uncontrollably, and then for that critical number of cycles, which for this model was about 37000, read the value of the critical length of the crack, which was about 11 mm. Then on the *J*-*Δa*, diagram Fig.12, for the displayed value of the critical crack length, the critical *J*-integral value is obtained (J_c=*55,921 mJ/mm*^{2}), and on the diagram SIF - number of cycles, Fig.13, for the displayed number of cycle, the critical stress intensity factor value is obtained (K_{Ic}=*2892,1 MPa mm*$^{1/2}$).

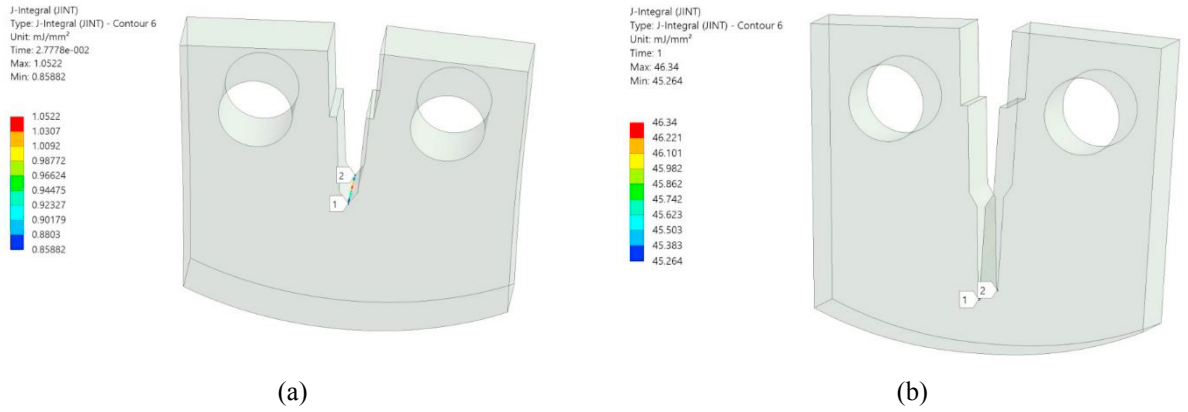

Figure 10. Values of *J*-integral of the specimen ($\boldsymbol{mJ/mm^2}$) for elevated temperature after crack opening (a) and at the end of crack propagation simulation (b)

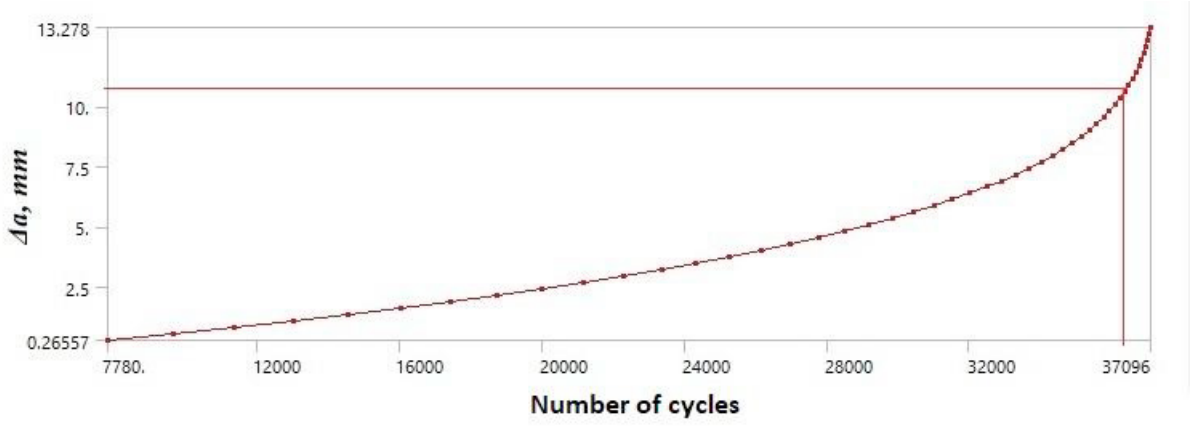

Figure 11. *a-N* diagram for a simulated specimen at HT

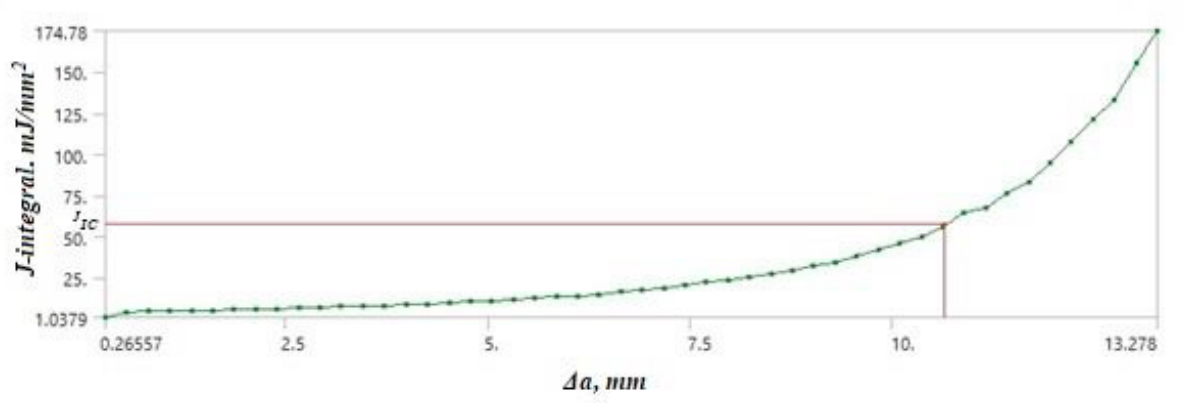

Figure 12. Numerically determined values of the critical J integral (J_c=*55,921 mJ/mm*^{2}) at HT

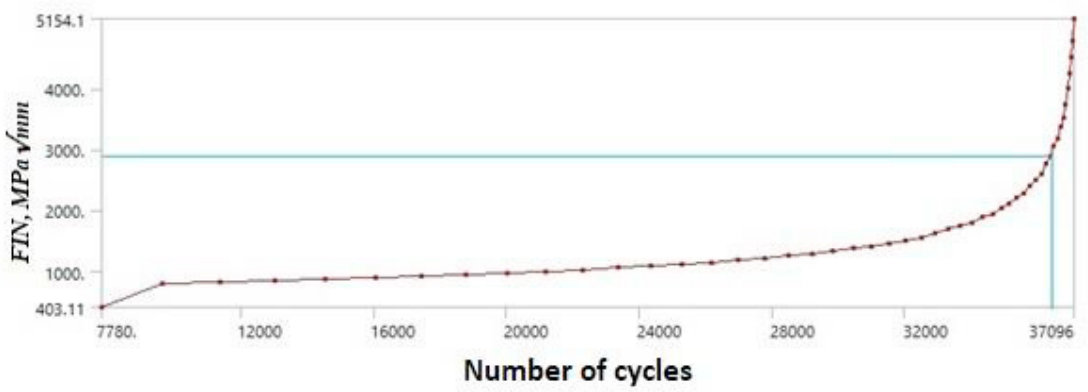

Figure 13. Numerically determined values of the critical SIF (K_{Ic}=*2892,1 MPa mm*$^{1/2}$)

2.2.Specimen for room temperature testing

The same procedure was repeated for the specimen tested at room temperature (RT). After defining the geometry according to the dimensions of specimen in the experiment, Figs. 2 and 14, the FE mesh has been defined, Fig. 4. Tetrahedral elements were also used in this model, where the total number of nodes for the model RT is 127116, while the number of elements is 88131.

.

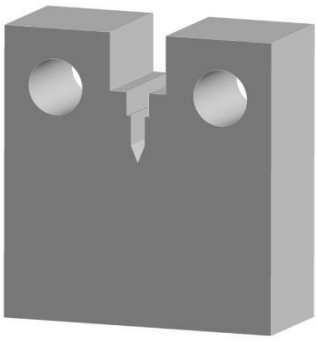

Figure 14. Geometry of the sample for testing at RT

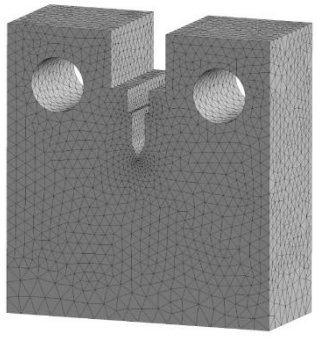

Figure 15. Mesh of tetrahedral elements

The boundary conditions corresponded to the experiment, and the maximum value from the experiment F=29833 N was taken, Fig. 16. Figs. 17-20 show the appearance of the displacement of the speciimen at the end of the numerical propagation simulation process, the stress state after the opening of the crack and at the end of the simulation (the maximum stress is at the tip of the crack in both cases), then changes in the *J*-integral value through the propagation steps. The value of the critical *J*-integral (J_c=*126,7 mJ/mm*^{2}) was numerically determined on the RT model, which can be seen in Fig. 21, as well as the value of the critical SIF, K_{Ic} (K_{Ic}=*3374,2 MPa mm*$^{1/2}$), Fig. 22.

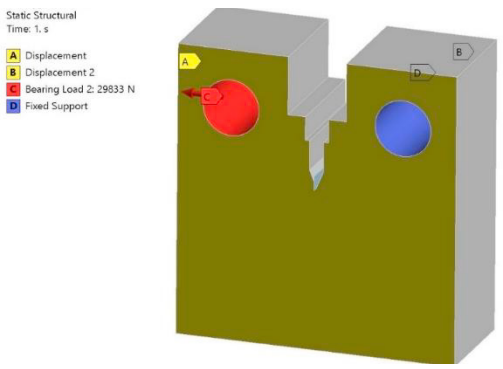

Figure 16. Boundary conditions (blue and yellow colors) and bearing load (red color)

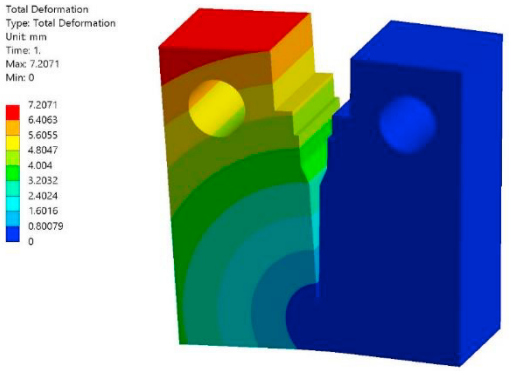

Figure 17. Specimen displacements at the end of the process of numerical simulation of crack propagation in specimen at RT

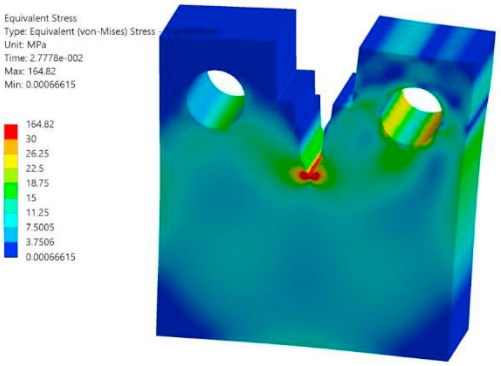

Figure 18. Stress state after crack opening

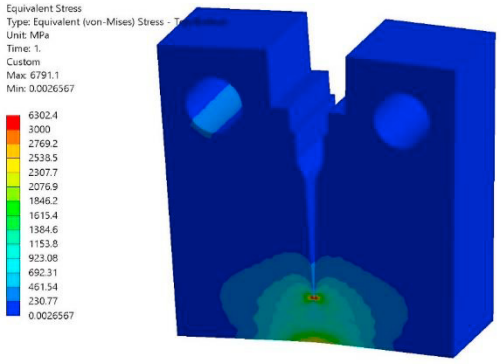

Figure 19. Stress state at the crack tip at the end of the simulation

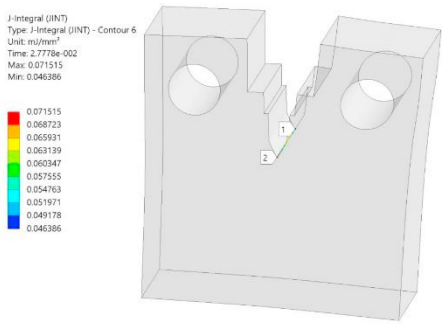

(a)

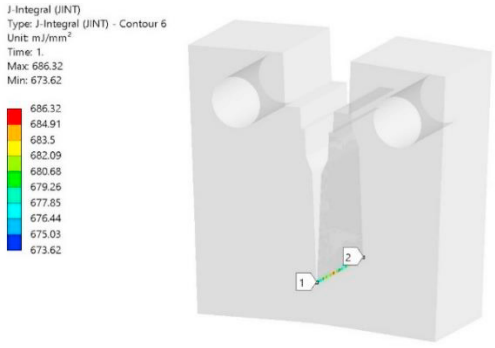

(b)

Figure 20. Changes in *J*-integral values in mJ/mm^2 through crack growth steps for specimen at RT

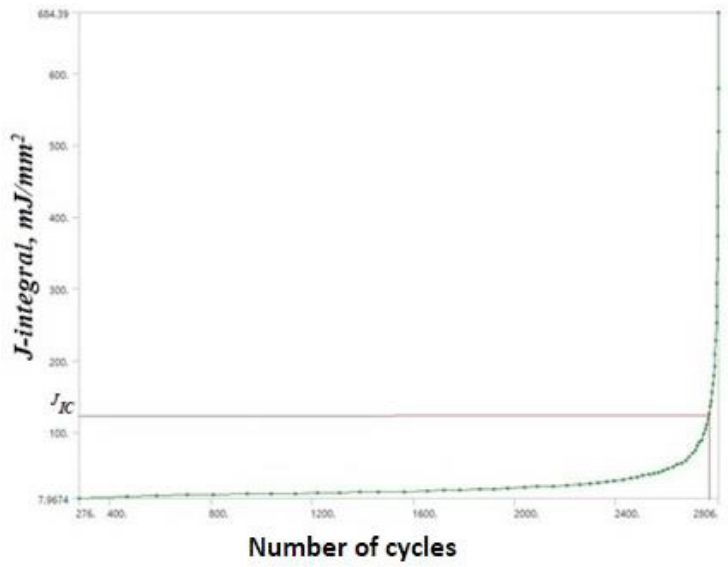

Figure 21. Numerically determined values of the critical *J* integral (J_c=*126,7 mJ/mm*^{2}) on the RT model

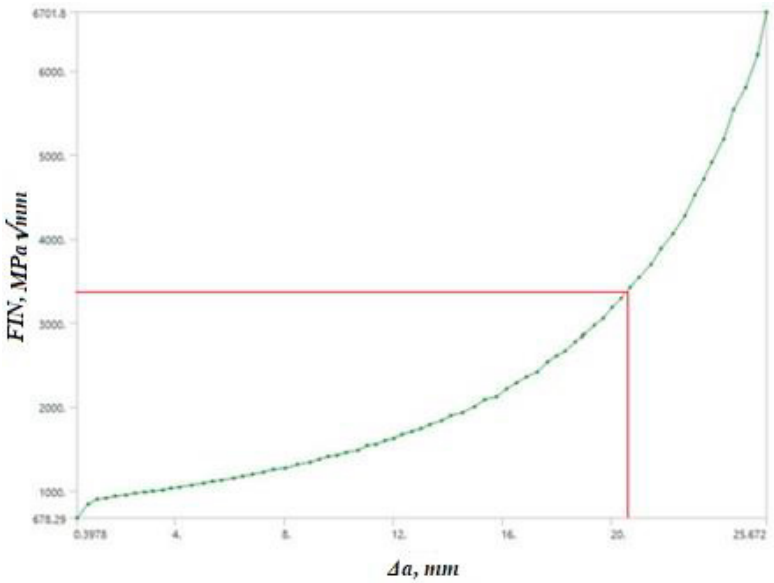

Figure 22. Numerically determined values of the critical SIF (K_{Ic}=*3374,2 MPa mm*$^{1/2}$) on the RT model

3. FEM fatigue crack growth prediction

Using the FEM, the basis of the numerical analysis that was made by the da/dN − ΔK curves is done, on the basis of which the coefficients of the Paris equation C and m were determined. Boundary conditions and loads are defined according to the experiment.

In the following part, the results of the simulation for two specimens, at service (HT) temperature and room (RT) temperature, will be presented. The results show the models themselves in a deformed shape, with stress and strain values, stress intensity factor (SIF) values, as well as obtained crack length diagrams - number of cycles for each model.

3.1 Specimen at elevated temperature

The geometry of the specimen is defined according to the dimensions of the specimen in the experiment, fig. 1 and 23. After defining the grids of finite elements, there followed the stages of defining boundary conditions and loads that corresponded to the experiment. In fig. 24 is shown the model after the action of the fatiguing load with the stress distribution in the vicinity of the crack tip. The values of SIF, K_I, from the opening to the final crack length, calculated for 36 steps of load application, are shown in fig. 25 (a) and (b). The value of the stress intensity factor was calculated at the nodes of the crack tip and it can be seen that the crack grew in the plane.

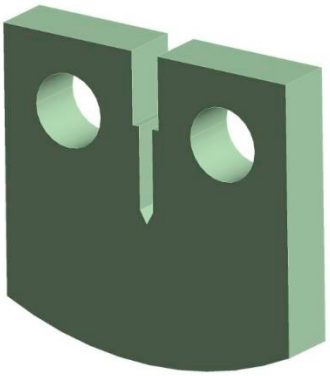

Figure 23. Geometry of the sample for testing at HT

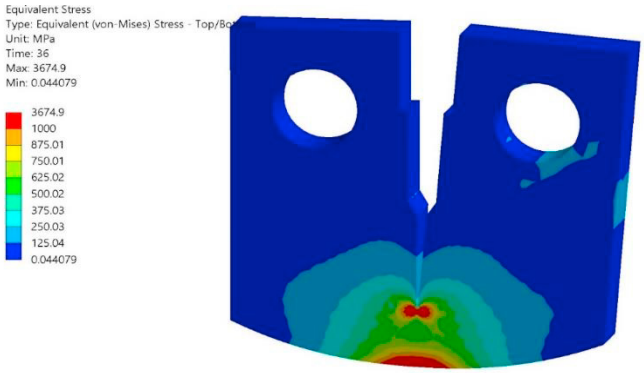

Figure 24. Stress distribution in MPa in the deformed model

The number of cycles until reaching the critical length of the crack, a_c, was N = 50130, which is almost the same value compared to the experimentally obtained cycle numbers, fig. 26.

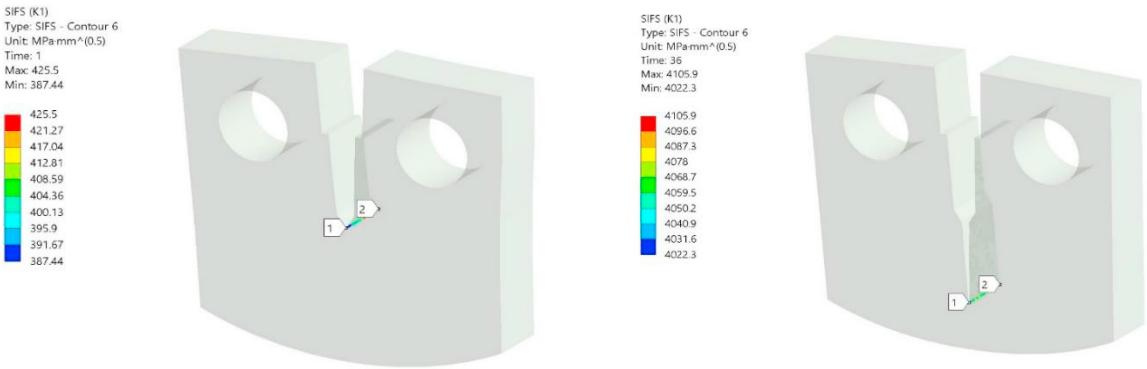

(a) (b)

Figure 25. SIF K_I values in MPa√mm, from: (a) opening to (b) final crack length for HT

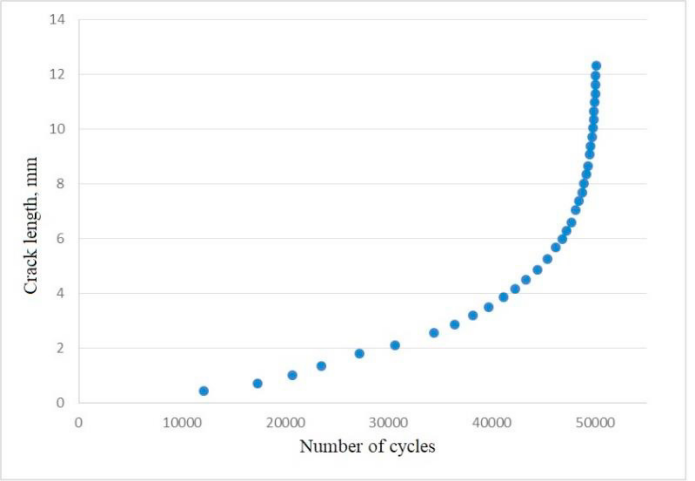

Figure 26. Diagram of dependence of a − N for the simulated specimen at HT

3.2. Specimen at room temperature

Exactly the same procedure was done for specimen model at room temperature. The geometry of specimen is defined according to the dimensions of specimen in the experiment, fig. 2 and 27. In fig. 28 is shown the appearance of the model after the fatigue loading with the stress distribution in the vicinity of the crack tip. The values of FIN, K_I, from opening to the final length of the crack are shown in fig. 29 (a) and (b).

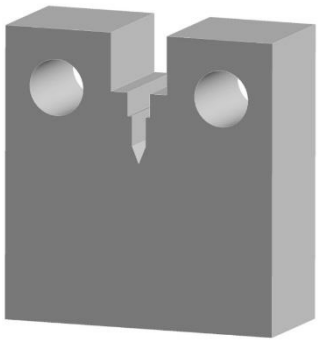

Figure 27. Geometry of the sample for testing at RT

Figure 28. Stress distribution in MPa in the deformed model

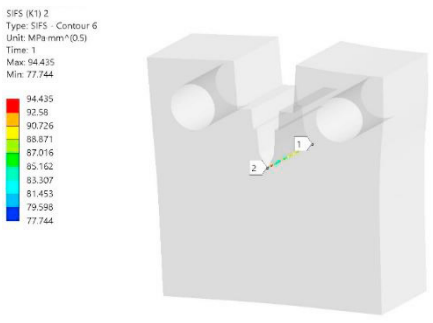

(a) (b)

Figure 29. SIF K_I values in MPa√mm, from: (a) opening to (b) final crack length for RT

The total number of cycles until reaching the critical crack length, a_c, on the RT model was N = 89623, which represents higher values compared to the experimentally obtained numbers of cycles at the corresponding crack lengths, fig. 30.

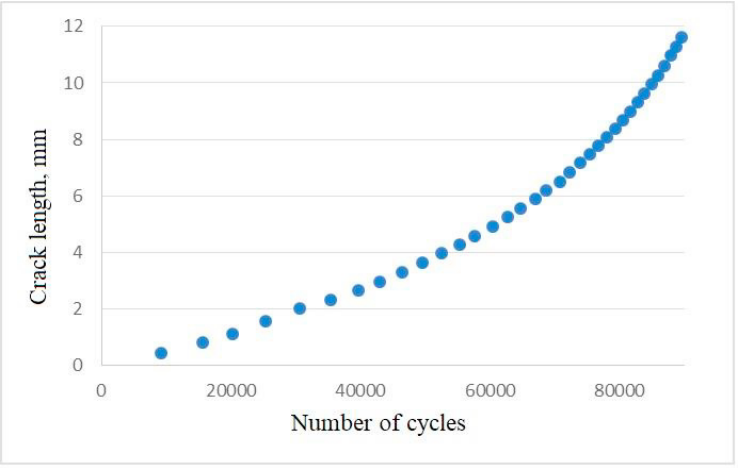

Figure 30. Diagram a - N for a simulated specimen at RT

4. Results of numerical analysis

4.1.Numerical calculation of J - integral and critical value of stress intensity factor

The numerically determined critical value of the J-integral in the case of a specimen for elevated (HT) temperature is J_{Ic}=55.921 kJ/m2 (65 kJ/m2 was obtained by experiment), and the numerically determined critical value of the stress intensity factor at elevated temperature (HT) is K_{Ic}=2892.1 MPa √mm = 91.45 MPa√m (99 MPa√m was obtained experimentally), tab. 1.

For specimen simulated at room temperature (RT), the numerically determined value of the critical J-integral is J_{Ic}=126.7 kJ/m2 (140 kJ/m2 was obtained by experiment), and the numerically determined value of the critical FIN was K_{Ic}=3374.2 MPa√mm = 106.7 MPa√m (174 MPa√m was obtained experimentally), tab. 2.

Table 1. Values of J_{IC} and K_{Ic} tested specimen at elevated temperature obtained by experiment and numerical simulation

540 °C	J_{IC}, kJ/m^2	K_{Ic}, MPa√m
Experiment	65	99
Numerical simulatiom	55.921	91.45

Table 2. Values of J_{IC} and K_{Ic} tested specimen at room temperature obtained by experiment and numerical simulation

18 °C	J_{IC}, kJ/m^2	K_{Ic}, MPa√m
Experiment	140	174
Numerical simulatiom	126.7	106.7

The obtained value for J_{Ic} is about 9% lower than in the experiment for specimen at RT, tab. 2, while for specimen at HT, the value obtained numerically is about 14% lower than the value obtained by experiment, tab. 1. The K_{Ic} value obtained by numerical simulation for HT is about 7.5% lower than the experimentally obtained value. In the case of RT, the K_{Ic} obtained by numerical simulation is about 38% lower than the experimentally obtained value, tab. 2. The differences can be explained by the imperfection of the numerical model used, which is based only on the elastic properties of the material, but in general the results of the numerical simulations can be considered satisfactory in terms of determining the direction of further research.

4.2. Numerical prediction of fatigue crack growth

Fig. 31 shows a comparison of *a-N* dependence curves obtained by experimental testing and numerical simulation of crack growth at HT, while in Fig. 32 can be seen the same comparison at RT. The values of the SIF in the case of the specimen HT for a crack length of 12.3 mm amounted to 4105.90 MPa√mm = 129.84 MPa√m, tab. 1., Fig. 25 (b), while the values of the SIF for a crack length of 11.5 mm in the case of the tested specimen RT reached the value of 301.51 MPa√mm = 9.53 MPa√m, tab. 2nd, Fig. 29 (b). The numerically simulated number of cycles required to reach the final length of the crack in the case of the HT specimen was obtained almost the same number of cycles in the numerical simulation (N_{num} = 50130 cycles and N_{exp} = 50300 cycles) as in the experiment, Fig. 31, while in the case of the specimen for RT it showed slightly higher values than the experimental results (N_{num} = 89623 cycles vs. N_{exp} = 72887 cycles) Fig. 32.

The number of cycles required to reach a certain crack length at RT in the case of numerical simulation is slightly higher than the number of cycles obtained. The slope of the curves at a lower number of fatigue cycles at RT (N ≈ 60000 cycles) is the same both in the case of experimental testing and in numerical simulation. When the number of fatigue cycles is further increased until the critical crack length is reached, the slope is slightly higher in the case of the experiment, which can be explained by the fact that the fatigue rate was higher in the experiment than in the simulation, which is a consequence of the microstructure of the material itself, which cannot be taken taken into account during numerical simulation. When simulating for HT, the slope of the curves was very similar and the *a-N* diagram largely corresponds to the experiment.

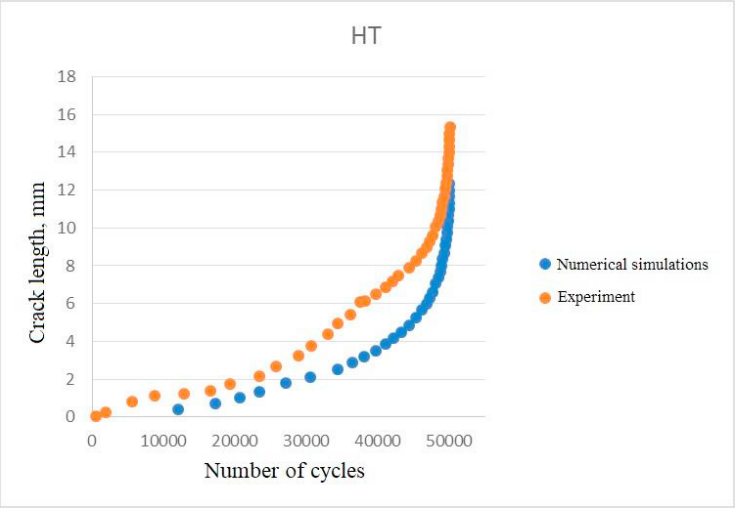

Figure 31. Comparison of experimental and numerical *a-N* curves of specimen HT

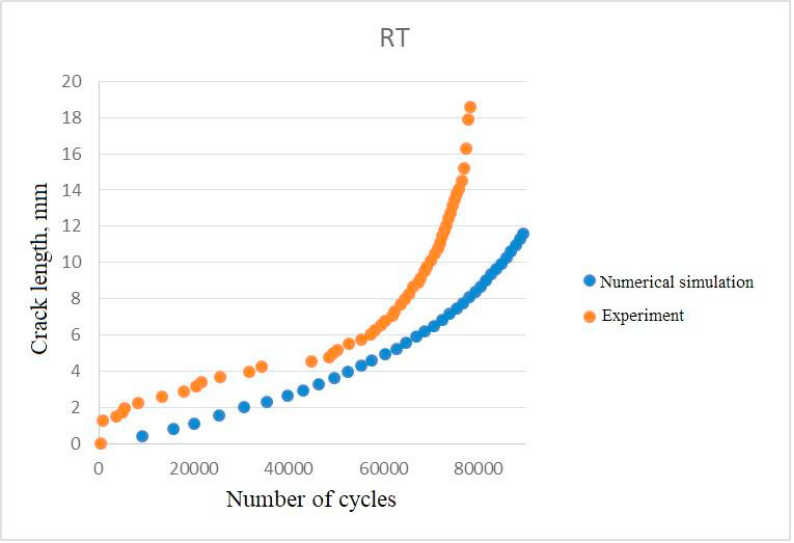

Figure 32. Comparison of experimental and numerical *a-N* curves of specimen RT

5. Conclusions

Numerical analysis was based on experimentally obtained results, primarily related to mechanical properties of materials, yield strength, tensile strength and Paris coefficients. The results obtained by numerical analysis showed a good agreement with the experimentally obtained *J*-integral results as well as the number of cycles for the specimen tested at room and elevated temperature. This verified the numerical approach to solving problems related to fatigue crack growth and the calculation of the critical *J*-integral value.
Further research should certainly go in the direction of a detailed examination of welded joints made of 14MOV6 3 steel grade and its behavior at elevated operating temperatures.

Acknowledgements

This work was supported by the Ministry of Education, Science and Technological Development of the Republic of Serbia (Contract No.451-03-68/2022-14/200135).

References

[1] M. Rakin et al, Application of the finite element method in materials engineering, Faculty of Technology and Metallurgy, Belgrade, 2014.
[2] A. M. Grbović, Investigation of fatigue life in superalloys structural components, Doctoral dissertation (IN Serbian), University of Belgrade, Faculty of Mechanical Engineering, Belgrade, 2012.
[3] D. D. Živojinović, Fracture mechanics aplication on integrity assesment of welded construction made from aluminum alloys, Doctoral dissertation (IN Serbian), University of Belgrade, Faculty of Mechanical Engineering, Belgrade, 2013.
[4] M. M, Grbović A, Software tools in design, Faculty of Mechanical Engineering, Belgrade, 2017.
[5] www.ansys.com
[6] Bojana V. Zečević, Effect of operating temperature on the resistance of low carbon microalloyed steel for thermal power plants to crack initiation and growth, Doctoral dissertation (IN Serbian), University of Belgrade, Faculty of Technology and Metallurgy, Belgrade, 2022.
[7] *Aleksić B. , Grbović A., Milović Lj. , Hemer A. , Aleksić V. :* Numerical simulation of fatigue crack propagation: A case study of defected steam pipeline*, Engineering Failure Analysis, Volume 106, December 2019. ISSN 1350-6307*

[8] *Hemer A., Milović Lj., Grbović A., Aleksić B., Aleksić V.:* Numerical determination and experimental validation of the fracture toughness of welded joints*, Engineering Failure Analysis, Volume 107, January 2020. ISSN 1350-6307*
[9] Aleksić B., Grbović A., Hemer A., Milović Lj., Aleksić V.: *Evaluation of Stress Intensity Factors (SIFs) Using Extended Finite Element Method (XFEM)*, In: Proceedings of the 17th International Conference on New Trends in Fatigue and Fracture, Eds: Ricardo R. Ambriz, David Jaramillo, Gabriel Plascencia and Moussa Nait Abdelaziz, Springer, 2018, 355-369.
[10] Aleksić V., Momčilović D., Aleksić B., Milović Lj., Sedmak A.: *Analysis of the steam line damages*, 12th International Conference on Accomplishments in Electrical and Mechanical Engineering and Information Technology DEMI 2015, Banja Luka, Republika Srpska, 29.05.-30.05. 2015, Zbornik radova na CD-u, 415-420.
[11] Aleksić B., Milović Lj., Grbović A., Hemer A., Aleksić V., Zrilić M.: *Experimental and numerical investigation of the critical values of J-integral for the steel of steam pipelines*, ECF 22-Loading and Environmental Effects on Structural Integrity, Serbia 2018, Procedia Structural Integrity 13, 2018, 1589-1594.